1986

A Computer Model of the Start-up Transients in a Vapor Compression Refrigeration System

H. Rajendran

M. Pate

A COMPUTER MODEL OF THE STARTUP TRANSIENTS IN A VAPOR-COMPRESSION REFRIGERATION SYSTEM

N. RAJENDRAN
and
MICHAEL B. PATE
Department of Mechanical Engineering
Iowa State University, Ames, Iowa (USA)

1. INTRODUCTION

The vapor-compression cycle, which is the most widely used cycle for refrigeration and air conditioning, frequently operates in a transient mode. Examples of transients are startup and shutdown surges, cycling, defrost, and formation of water, ice, or frost. Therefore, transients are important for the proper design of refrigeration and air conditioning system components.

The goal of the present work was to develop a computer program for simulating the startup transient behavior of a vapor-compression system and to analyze a typical test case using the program. In the future, the computer model can be expanded to include other transients such as frost formation and shutdown. It can also be combined with the dynamic simulation of a building for the purpose of investigating transient interactions between refrigeration systems and buildings.

2. OVERALL APPROACH

The transient model of a vapor-compression system developed herein includes component models for the condenser, evaporator, compressor, expansion device, and accumulator, as shown in Fig. 1. The refrigerant in each component is modeled as a lumped-mass system with a single node representing each phase region. Both of the air-to-refrigerant heat exchangers are the circular tube-continuous fin type. The compressor is assumed to be a hermetically sealed, reciprocating type with the compressor and the compressor shell being modeled as two separate control volumes. The process of compression is assumed to be adiabatic with the exponent of compression, k, being calculated as a function of the inlet temperature. The expansion device is a thermostatic expansion valve that is assumed to be adiabatic. Heat capacity effects in the walls of the heat exchangers, accumulator, and compressor are modeled using lumped-mass systems represented by single nodes and constant specific heats.

Conservation equations for mass and energy were written in differential form for the refrigerant in the accumulator, the compressor shell, and each heat exchanger. Energy equations were also written for the structural material in each of the above components. Since pressure drops were neglected in the heat exchangers, the mass and energy equations, along with the mass flow rate equations for the expansion device and compressor, describe the temporal behavior of the complete system. Property relations and correlations to evaluate heat transfer coefficients complete the set of model equations. Numerical methods were used to solve the set of ordinary differential equations.

3. COMPARISON OF MODELS

The model presented in this study can be compared with five other transient models of complete vapor-compression systems as shown in Table I. The five models were developed by Chi and Didion /1/, Dhar and Soedel /2/, MacArthur /3/, and Murphy and Goldschmidt /4,5/. Two separate models were reported in the latter study, one for shutdown and the other for startup. The present model combines many of the features presented in these earlier models while introducing several new features. However, it is important to note that the authors of the present model did not necessarily try to develop the most complete model but rather a model that represented, in their judgment, a balance between comprehensiveness (which can result in improved accuracies) and simplicity (which can reduce the computer time and convergence difficulties). For example, unlike the Chi and Didion model /1/, the present model neglects the dynamic responses of the electric motors, shafts, and electric fans in order to reduce the computer program length and computing time. The present model has also been developed with a minimum of reliance on experimental data so that it can be used to analyze new systems. For example, the Dhar and Soedel model /2/ calculates the mass flow rates between the evaporator, the accumulator,

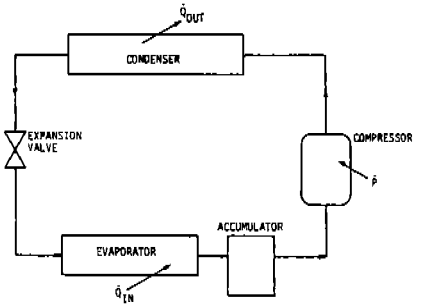

Fig. 1 - Typical vapor-compression cycle.

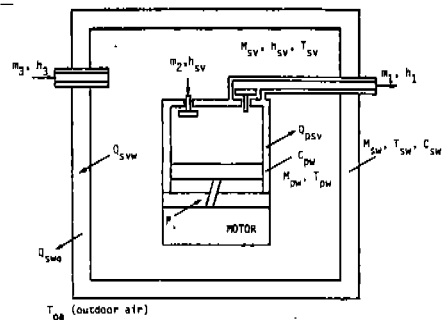

Fig. 2 - Compressor and compressor shell.

TABLE I. Comparison of models.

Model	Transients Modeled	Operation Mode	Components Modeled	Oil in Shell	System Size, kW	Type of Expansion Device	Nodes in HX	ΔP in HX	Comparison with Experiment
Chi & Didion /1/	Startup shutdown	Heating	All	No	14.1	TEV	Single	Yes	Yes
Dhar & Soedel /2/	Startup shutdown	Cooling	All	Yes	2.3	TEV	Single	No	No
MacArthur /3/	Startup shutdown	Heating	All	No	10.5	TEV	Multiple	No	No
Murphy & Goldschmidt (A) /4/	Shutdown	Cooling	All except compressor	No	10.5	Capillary tube	Single	No	Yes
Murphy & Goldschmidt (B) /5/	Startup	Cooling	All except evaporator	No	10.5	Capillary tube	Single	No	Yes
Present	Startup	Cooling	All	No	10.5	TEV	Single	No	No

HX--Heat exchanger.
TEV--Thermostatic expansion valve.

and the compressor, using empirical relations developed by them. The present model also uses a thermostatic expansion valve (TEV) instead of the capillary tube that was modeled by Murphy and Goldschmidt /4,5/. Another difference between this new model and some past models is that in the formulation of the energy equation for the refrigerant inside each component, the term Mvdp/dt has been considered. Specifically, even though the MacArthur model /3/ considered several nodes in the heat exchangers, thus adding sophistication to the model, it did not consider the effects of this term. It should be noted, however, that this term is important only for severe transients, which occur for only a short period immediately after startup.

4. COMPRESSOR

A schematic of the compressor within the hermetic shell is shown in Fig. 2. Equations to calculate the mass flow rate and the state of the vapor leaving the compressor are derived and discussed below. The mass flow rate in the compressor is given by /6/

$$m_1 = V_d N \eta_v / v_{sv} \tag{1}$$

The rate of work done on the vapor in the compression chamber is calculated from /7/

$$P = -0.185(k/(k-1))V_d N \eta_v p_s \left(1 - (R_p)^{(k-1)/k}\right) \tag{2}$$

The specific enthalpy of the vapor leaving the compressor is obtained from an energy balance on the vapor in the cylinder. This balance neglects heat transferred from the compressor cylinder walls and reheating from the cylinder head as follows:

$$h_1 = h_{sv} + P/m_1 \tag{3}$$

The temperature of the refrigerant vapor leaving the compressor cylinder is then calculated from property equations knowing the specific enthalpy and the pressure in the condenser /8,9/. The compressor friction and electric motor losses are assumed to be converted to heat and then absorbed by the compressor wall, which then loses heat by natural convection to the surrounding vapor. An energy balance on the compressor wall yields the equation for the wall temperature:

$$dT_{pw}/dt = (P_{\ell} - Q_{psv})/(M_{pw}C_{pw}) \tag{4}$$

The compressor shell houses the compressor and serves as a reservoir for the oil, which is used to lubricate the piston-cylinder assembly. The effects of oil in the compressor shell are considered to be outside the scope of this study and, as such, have been neglected. The pressure in the compressor shell is assumed to be representative of the pressure in the entire low-pressure side of the refrigeration system. Figure 2 shows the mass flow of refrigerant from the accumulator into the compressor shell and from the shell into the compressor cylinders. Also shown are heat transfer rates from the vapor to the wall and from the wall to the air. Mass and energy balances on the vapor in the shell yield

$$dM_{sv}/dt = m_3 - m_1 \tag{5}$$

$$d(M_{sv}u_{sv})/dt = m_3h_3 - m_1h_{sv} + Q_{psv} - Q_{svw} \tag{6}$$

Using the definition of enthalpy, these equations can be combined and then used to calculate specific enthalpy as follows:

$$M_{sv}dh_{sv}/dt = m_3(h_3 - h_{sv}) + Q_{psv} - Q_{svw} + M_{sv}v_{sv}dp_s/dt \tag{7}$$

The state of the vapor is thus defined, since the specific volume of the vapor in the shell can be calculated from the total volume of the compressor shell as follows:

$$v_{sv} = V_s/M_{sv} \tag{8}$$

The temperature of the shell wall can be calculated from an energy balance on the wall assuming that heat transfer is by natural convection:

$$M_{sw}C_{sw}dT_{sw}/dt = Q_{svw} - Q_{swa} \tag{9}$$

5. EXPANSION VALVE

A thermostatic expansion valve (TEV) was modeled in this study, since it is one of the most common types of expansion devices used in the refrigeration industry. The expansion valve attempts to maintain the refrigerant that leaves the evaporator at a constant superheat, ensuring that only vapor enters the compressor through the suction line. Therefore, the mass flow of refrigerant through the TEV is a function of the vapor superheat at the exit of the evaporator and the pressure difference across the valve. In this study, the TEV has been modeled as an adiabatic, variable-area orifice (similar to the expansion valve modeled by Dhar and Soedel /2/). The refrigerant entering the orifice can be a vapor, liquid, or a combination of the two phases, depending upon the conditions at the exit of the condenser. If the refrigerant entering the valve is a vapor and the flow is not choked, the mass flow rate is /2/

$$m_t = 8640p_dA_x(2kg((p_s/p_d)^{2/k} - (p_s/p_d)^{(k+1)/k})/((k - 1)RT_t))^{1/2} \tag{10}$$

During choked conditions, the mass flow rate is given by /2/

$$m_t = 8640p_dA_x(2kg((R_c)^{2/k} - (R_c)^{(k+1)/k}))^{1/2} \tag{11}$$

where the isentropic exponent, k, is assumed to be a constant, and R_c is

$$R_c = (2/(k + 1))^{k/k-1}$$

The mass flow rate when the refrigerant entering the valve is all liquid, or, a mixture of liquid and vapor, is calculated from /10/

$$m_t = 720 C_d A_x (2g(p_d - p_s)/v_t)^{1/2} \tag{12}$$

where the coefficient of discharge, C_d, is given by

$$C_d = 0.0802(\rho_{te})^{1/2} + 0.396 v_t \tag{13}$$

An energy balance on the expansion valve results in an isenthalpic process. In the above equations, the valve port area is a function of the superheat of vapor at the exit of the evaporator as follows:

$$A_x = A_{ss} - G(\Delta T_{ss} - \Delta T_{sb}) \tag{14}$$

This equation is based on a proportional-gain type of controller /11/. It should be noted that the proportional-gain controller introduces a steady-state error which could be eliminated by adding integral gain. The superheat sensed by the bulb is

$$\Delta T_{sb} = T_b - T_{el} \tag{15}$$

where the temperature of the thermobulb wall is calculated from an energy balance:

$$dT_b/dt + T_b/\tau_b = T_{evw}/\tau_b \tag{16}$$

where τ_b $(= M_b C_b / U_b A_b)$ is the time constant of the thermobulb temperature response.

6. CONDENSER

An air-cooled, forced-draft type of condenser has been modeled in this study. Depending upon the rate of heat transfer from the refrigerant to the condenser wall, the condenser contains superheated vapor, a mixture of saturated vapor and saturated liquid, and subcooled liquid. To accommodate these refrigerant conditions in the condenser, three different models were developed for the condenser. Chi and Didion /1/ and Dhar and Soedel /2/ used a similar approach.

Superheated Refrigerant Model. A sketch of the superheated refrigerant model is shown in Fig. 3. Mass and energy balances, similar to Eqs. (5) and (6) for the compressor shell, can be written for the vapor in the control volume as follows:

$$dM_{cv}/dt = m_l - m_t \tag{17}$$

$$d(M_{ev} u_{cv})/dt = m_l h_l - m_t h_t - Q_{cvw} \tag{18}$$

These two equations can be combined to form an equation for calculating specific enthalpy:

$$M_{cv} dh_{cv}/dt = m_l(h_l - h_{cv}) - m_t(h_t - h_{cv}) + Q_{cvw} + M_{cv} v_{cv} dp_d/dt \tag{19}$$

The mass flow rate into and out of the condenser is equal to the mass flow through the compressor and expansion valve, respectively. The specific volume of the vapor can be found knowing the mass of vapor and the condenser volume. The temperature and the pressure in the condenser can then be calculated from property relations. The condenser wall temperature is calculated from an energy balance on the condenser wall similar to the procedure used in Eq. (9) for the wall of the compressor shell. The standard Dittus-Boelter equation was used to calculate the heat transfer coefficient on the inside of the tubes. For heat transfer from the outside fins to the air, the heat transfer coefficient was obtained from correlated data for circular tube-continuous fin heat exchangers given by Kays and London /12/.

Saturated Refrigerant Model. As heat transfer from the refrigerant vapor to the condenser wall occurs, the superheat of the vapor decreases so that eventually the refrigerant vapor becomes saturated. When this occurs, a saturated refrigerant model is adopted for the condenser. This model neglects the effects of the super-

heat region and assumes that the entire condenser is filled with saturated refrigerant. Even though a schematic of the saturated model is not shown, it would be similar to the saturated part of the subcooled refrigerant model, which is shown in Fig. 4 and discussed in the next section. Mass and energy equations for the saturated refrigerant can be written as before where the specific enthalpy of the refrigerant mixture is calculated from the combined energy and mass equation. The saturated refrigerant model requires an assumption regarding the variation of quality in the condenser. Therefore, a linear variation of quality was assumed along the length of the tube. This variation represents a balance between simplifying the model and representing the actual situation in the condenser. The specific volume of the saturated refrigerant can be calculated from the condenser mass and volume as before. With two properties known, namely, the specific volume and the specific enthalpy, the remaining properties, such as the pressure and the bulk quality, can also be found. The temperature of the saturated vapor and liquid refrigerant are equal and can be found from appropriate property relations. The wall temperature can be calculated from an energy balance on the wall of the condenser where the Nusselt number for condensation in a horizontal tube was calculated from a correlation proposed by Akers and Rosson /13/.

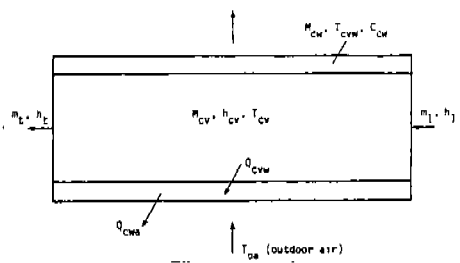

Fig. 3 - Superheated vapor condenser model.

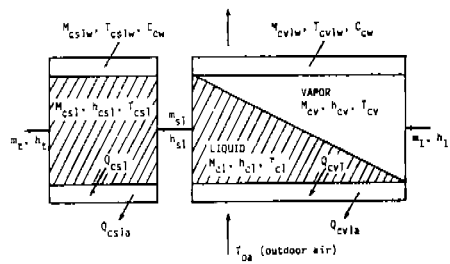

Fig. 4 - Subcooled refrigerant condenser model.

Subcooled Refrigerant Model. The subcooled-liquid model of the condenser is shown in Fig. 4. The condenser consists of two control volumes, one with a mixture of saturated vapor and liquid, and the other with subcooled liquid only. The subcooled region is near the exit of the condenser, downstream of the saturated region. Governing differential equations were derived for the condenser by applying mass and energy balances to the saturated and subcooled regions. The resulting equations are similar to those derived for the superheated condenser model, except that a new term that defines the rate of work done at the moving boundary between the saturated and subcooled refrigerant control volumes appears in the energy equation. This is illustrated in the energy equation for the mixed refrigerant region:

$$d(M_{cvl}u_{cvl})/dt = m_l h_l - m_{sl}h_{sl} - Q_{cvl} - p_d d(M_{cvl}v_{cvl})/dt \qquad (20)$$

where $p_d d(M_{cvl}v_{cvl})/dt$ is the new work term. Combining the mass and energy equations results in

$$M_{cvl}dh_{cvl}/dt = m_l(h_l - h_{cvl}) - m_{sl}(h_{sl} - h_{cvl}) - Q_{cvl} + M_{cvl}v_{cvl}dp_d/dt \qquad (21)$$

The mass of the refrigerant in the condenser is related to the total condenser volume as

$$M_{cvl}v_{cvl} + M_{csl}v_{cs} = V_c \qquad (22)$$

Since the compressibility of liquid is low, the specific volume of the subcooled liquid is assumed to be the same as that of the saturated liquid in the condenser. Since the average quality of the refrigerant in the saturated region is 0.5, the mass flow rate of liquid from the saturated to the subcooled region, m_{sl}, and the pressure, P_d, are solved for with Eq. (21) and (22). The specific enthalpy of the subcooled liquid can be found from the energy equation for the subcooled liquid region where the inside heat transfer coefficient is evaluated from the Dittus-Boelter equation. The length of each region is calculated knowing the volume of the region and the cross-sectional area of the tube.

7. EVAPORATOR

The evaporator was a dry-expansion type (DX) that was modeled as a fin and tube heat exchanger. At the time of startup, the evaporator is completely filled with saturated refrigerant, which is mostly in the liquid phase since the evaporator is at a lower temperature than the condenser. The system is designed so that at steady state low-quality refrigerant enters the evaporator from the expansion valve while the refrigerant vapor leaving the evaporator is superheated to 3° to 7° C. The evaporator is assumed to contain two regions: (1) saturated where the heat transfer is two-phase forced convection boiling and (2) superheated where the heat transfer is single-phase forced convection. The vapor and the liquid in the evaporator are assumed to be two separate control volumes characterized by single valued properties (i.e., the control volumes are assumed to behave as stirred tanks) as shown in Fig. 5. Prior to startup the vapor and the liquid phases of the refrigerant are both saturated. After startup, heat transfer to the refrigerant vapor results in a superheated condition near the exit. The liquid in the evaporator is assumed to be saturated at all times. Pressure drops have been neglected so that the pressure in the evaporator is uniform and equal to the pressure in the accumulator and the compressor shell. Dhar and Soedel /2/ follow a similar procedure in their model of the evaporator.

The mass balance on the vapor and liquid control volumes, respectively, results in

$$dM_{ev}/dt = x_{te}m_{te} + m_e - m_4 \tag{23}$$

$$dM_{el}/dt = (1 - x_{te})m_{te} - m_e - m_5 \tag{24}$$

The energy balance on the vapor gives

$$d(M_{ev}u_{ev})/dt = x_{te}m_{te}h_{te} + m_eh_{eg} - m_4h_4 + Q_{ewv} - p_s d(M_{ev}v_{ev})/dt \tag{25}$$

which can be rewritten when combined with the mass balance equations:

$$M_{ev}dh_{ev}/dt = x_{te}m_{te}(h_{eg} - h_{ev}) + m_e(h_{eg} - h_{ev}) - m_4(h_4 - h_{ev}) + Q_{ewv} + M_{ev}v_{ev}dp_s/dt \tag{26}$$

Similar equations can be derived for the liquid in the evaporator. In addition, an equation that relates the mass and specific volume of the refrigerant to the total volume of the evaporator coil can also be derived. A linear quality profile between the inlet and the exit of the evaporator was assumed. Energy equations were written for the evaporator wall with separate equations being formulated for the saturated refrigerant and the superheated vapor regions. The heat transfer from the wall to the saturated refrigerant is by two-phase convection boiling; whereas, the heat transfer from the wall to the superheated vapor is by single-phase forced convection. The two-phase heat transfer coefficient is calculated using the correlation proposed by Kandlikar /14/. As in the case of the condenser, the air-side heat transfer coefficient was calculated using correlated data /12/.

8. ACCUMULATOR

Suction-line accumulators are used in many split-system, vapor-compression systems. The accumulator prevents suction vapor from carrying slugs of liquid to the compressor and also functions as a reservoir to hold a percentage of the total system charge. In this study, the vapor in the accumulator is assumed to remain saturated in the presence of liquid, and superheated vapor forms only when the liquid refrigerant has completely evaporated. Two models, namely, a saturated refrigerant model and a superheated refrigerant model, are developed in this study.

Saturated Refrigerant Model. Figure 6 shows a schematic of the saturated refrigerant model of the accumulator. Both liquid and vapor phases enter the accumulator from the evaporator when the quality at the exit of the evaporator is less than unity. Under all conditions, only vapor is assumed to leave the accumulator. Mass balances on the vapor and liquid phases in the accumulator result in

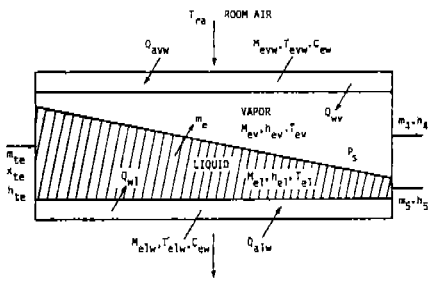

Fig. 5 - Evaporator model.

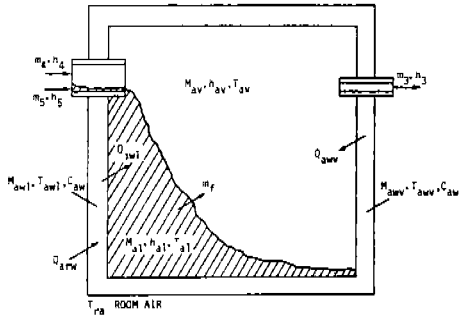

Fig. 6 - Saturated refrigerant accumulator model.

$$dM_{av}/dt = m_4 + m_f - m_3 \tag{27}$$

$$dM_{al}/dt = m_5 - m_f \tag{28}$$

while an energy balance on the vapor and liquid phases gives

$$M_{av}dh_{av}/dt = m_4(h_4 - h_{av}) + Q_{awv} + M_{av}v_{av}dp_s/dt \tag{29}$$

$$M_{al}dh_{al}/dt = Q_{awl} - m_f(h_{av} - h_{al}) + M_{al}v_{al}dp_s/dt \tag{30}$$

Since the pressure is known, the mass rate of liquid that is converted to vapor is obtained by combining the two energy balance equations:

$$m_f = (m_4(h_4 - h_{av}) + Q_{awv} + Q_{awl} - M_{av}dh_{av}/dt - M_{al}dh_{al} + V_a dp_s/dt)/(h_{av} - h_{al}) \tag{31}$$

The mass flow rate of saturated vapor out of the accumulator can be calculated from the volume equation for the accumulator and the mass balance equations. An energy balance can also be written for the wall of the accumulator assuming heat transfer is by natural convection.

Superheated Refrigerant Model. The superheated refrigerant model of the accumulator is similar to the saturated model shown in Fig. 6, except that the liquid phase is nonexistent and the vapor is superheated. Mass and energy equations can be written for the vapor in the accumulator as before.

9. SOLUTION SCHEME

The model of the overall refrigeration system consists of a set of differential and ordinary algebraic equations. The differential equations were solved numerically using an explicit finite-difference method. The time step was determined by a simple trial-and-error procedure called "interval-halving." In this method, the solution is first carried out for some value of Δt. This Δt is then reduced by halving and the system of equations is solved again. This is continued until two consecutive results agree to within a desired accuracy level. The computer simulation of the model was performed on a main-frame, digital computer using FORTRAN. The computer program consisted of a main program and separate subroutines for each system component, refrigerant property and heat transfer coefficient. Component subroutines were called by a main program in the following order: compressor, expansion valve, condenser, evaporator, accumulator, and compressor shell. In addition, several components, such as the condenser and accumulator, were described by multiple subroutines that represented different state models. The system was assumed to start from a position of equilibrium, with the pressure being the same throughout the system. Once the initial values at $t = 0$ were known, each subroutine evaluated the various variables at time $t + \Delta t$. This process was repeated until the system reached either the specified solution time or steady state.

10. RESULTS

A 10.5-kW (3-ton) nominal capacity, air conditioning unit with R-22 as the working fluid was simulated using the developed model. The test run simulated 15 minutes (real time) of operation after startup. The components were sized based on product literature from a heat pump manufacturer. Additional information concerning actual sizes of components can be found in /15/. Typical values of outdoor and indoor temperatures (35° C and 21° C, respectively) were chosen. An incremental time-step value of 0.001 minutes was selected based on the stability considerations discussed earlier. Some sample output is presented and discussed below. Most of this output is only for the first minute of the transient, because changes after this time were quite minor for most parameters. The one exception, though, is the drying out of the accumulator, which continues for a 12.5-min period. Several additional system parameters have not been reported here, even though they were available from the model. Examples of this output are mass inventory, wall temperatures, refrigerant quality and temperature, and energy transfer rates. A direct comparison of the results of this model with either experimental data or other models was not feasible due to differences in unit and component sizes.

System Pressures. Suction and discharge pressure transients are shown in Fig. 7 for the first minute only, for those reasons discussed above. In fact, after the first minute, the suction pressure showed negligible change, while the discharge pressure increased less than 40 kPa over a 12-min period. The steady-state values of the suction and discharge pressure were 588 kPa and 1740 kPa, respectively. The models compared earlier in this study predicted similar trends in the pressure curves. All the investigators reported rapid changes in pressure during the first minute and then steadying pressures immediately thereafter.

Mass Flow Rate. Figure 8 shows transients in the mass flow rates at the outlet of each component during the first minute. At steady state the mass flow rate was 3.9 kg/min. Figure 8 also shows that the compressor's mass flow rate jumps to its maximum value immediately after startup, which is to be expected for a constant motor speed assumption. A decreasing density at the suction of the compressor causes the mass flow rate to decrease as it approaches its final value. Trends similar to these have been observed by other investigators.

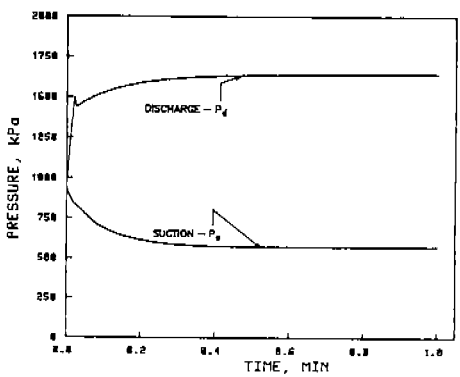

Fig. 7 - Suction and discharge pressure change during the first minute.

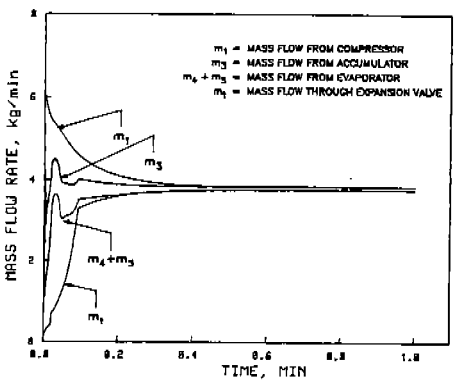

Fig. 8 - Refrigerant mass flow rates during the first minute.

Refrigerant Mass Inventory in the System. Refrigerant migration to the low-pressure side of the system during the off cycle is initially due to the pressure gradient caused by the compressor. After shutoff, the temperature gradient between the condenser and the evaporator drives the refrigerant to the low-pressure side. Therefore, prior to startup most of the refrigerant resides in the evaporator, the accumulator, and the compressor shell. Immediately after startup, the mass of refrigerant in each component changes rapidly as the compressor displaces the refrigerant from the low- to the high-pressure side of the system. A mass inventory in the system prior to startup and at steady state, as a percent of total charge, is as follows:

Component	Pre-startup	Steady State
Condenser	7.8%	71.5%
Evaporator	27.2%	5.5%
Accumulator	38.3%	5.3%
Compressor shell	26.7%	17.7%

Similar observations have been made by Mulroy and Didion /16/ in the experiments they conducted on a residential, split-unit air conditioner. The models developed by the other investigators also predict similar behavior of refrigerant migration.

Refrigerant Mass Inventory in the Accumulator. Figures 9 and 10 show the mass of liquid and vapor refrigerant in the accumulator during the startup transient. Prior to startup, the accumulator contains 0.602 kg of liquid and 0.145 kg of vapor refrigerant in the saturated condition. At approximately 3 seconds after startup, the accumulator charge reaches a maximum after which both the vapor and liquid mass show a decrease. At 12.5 minutes after startup, the accumulator dries out as all the liquid evaporates. The system proceeds to reach steady state immediately thereafter. Chi and Didion /1/ and Dhar and Soedel /2/ also observed for their models and systems that the accumulator trapped a large quantity of the refrigerant immediately after startup, and steady state was not reached until after the accumulator had dried out. These observations were also confirmed in experiments by Mulroy and Didion /16/.

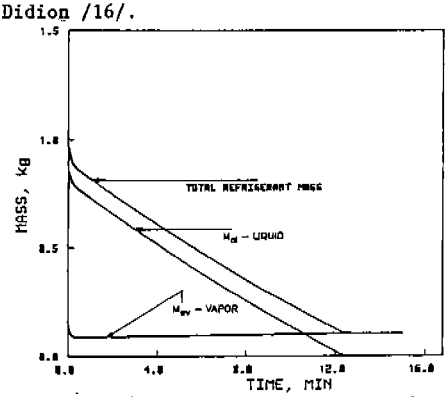

Fig. 9 – Refrigerant mass inventory in the accumulator.

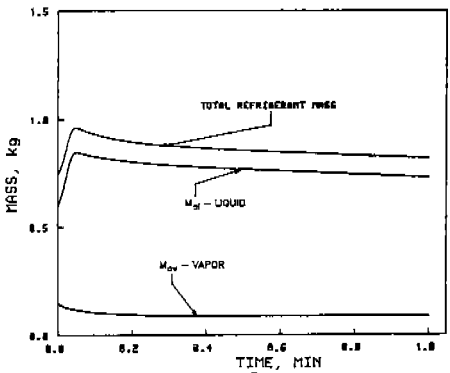

Fig. 10 – Refrigerant mass inventory in the accumulator during the first minute.

Superheat at Exit of Evaporator. Figure 11 shows the superheat of the vapor at the exit of the evaporator. After an initial increase to 6.2° C over a 16-sec period, the superheat slowly drops to a steady-state value of 3.7° C. A different setting of the expansion valve would have resulted in a different value of superheat at the exit of the evaporator.

Coefficient of Performance. The system coefficient of performance (COP) as a function of time is plotted in Fig. 12. The COP increases to a maximum value of 7.0 during the first 3 seconds of operation. After 3 seconds, the COP decreases and then increases again to a steady-state value of 5.6.

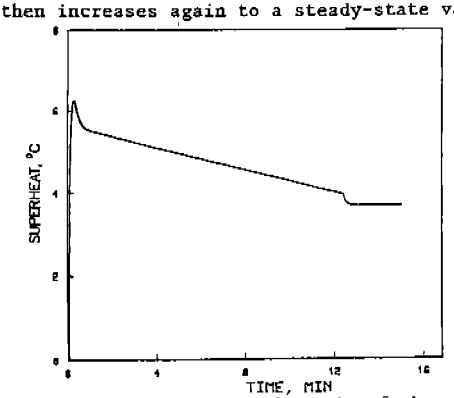

Fig. 11 – Superheat at the exit of the evaporator.

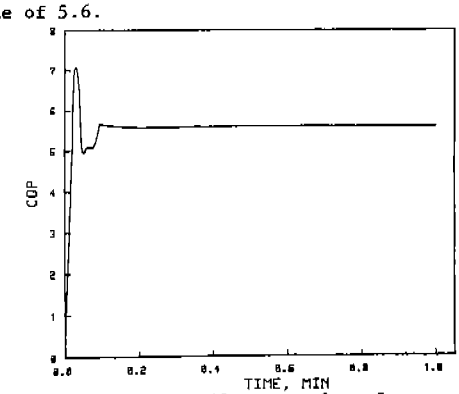

Fig. 12 – Coefficient of performance during the first minute.

11. SUMMARY

A computer model of the startup transient in a vapor-compression refrigeration system was developed using conservation of mass and energy equations in various components. A test run of the computer program was presented, and the results were consistent with the expected behavior of the system based on comparisons with past models and the limited experimental data available. Rapid fluctuations in the system variables occurred immediately after startup. The system reached steady state at approximately 12.5 min and only after the liquid in the accumulator had dried out. Refrigerant migration from the low- to the high-pressure side of the system immediately after startup was observed. This migration was consistent with experimental observations. These and other observations support the conclusion that a simple transient model can predict the dynamic behavior of a vapor-compression cycle during startup.

Several possibilities exist for improving the model. The number of nodes in the evaporator and condenser control volumes could be increased, and the momentum equation could be used to evaluate the frictional pressure drop in the heat exchangers and connecting pipes. Additional effects that could be considered are oil in the compressor shell, connecting lines in the system, and a variable motor speed for the compressor. Finally, the startup model presented in this study could be modified to include a shutdown transient.

NOMENCLATURE

A	area, m^2
C	specific heat, kJ/kg · °K
g	acceleration of gravity, m/s^2
G	gain of expansion valve, $m^2/°C$
h	specific enthalpy, kJ/kg
k	specific heat ratio
m	mass flow rate of refrigerant, kg/min
M	mass, kg
N	speed of compressor motor, rpm
p	pressure, kPa
P	rate of work done on the vapor refrigerant in compressor, kW
P_ℓ	rate of heat loss from motor, kW
Q	heat transfer rate, kW
R	gas constant, kJ/kg · °K
R_p	ratio of discharge pressure to suction pressure
T	temperature, K
u	specific internal energy, kJ/kg
U	heat transfer coefficient, kW/m^2 · °K
v	specific volume, m^3/kg
V	volume, m^3
x	quality

Subscripts

a	accumulator
b	thermobulb
c	condenser
d	discharge
e	evaporator
g	superheated vapor refrigerant
l	saturated liquid refrigerant
p	compressor
r	room
s	compressor shell; suction
sb	superheat sensed by thermobulb
ss	steady-state value
t	refrigerant leaving condenser
te	refrigerant leaving expansion valve
v	saturated vapor refrigerant
w	wall
x	expansion valve
1	refrigerant leaving compressor
2	refrigerant leaving compressor shell
3	refrigerant leaving accumulator
4	vapor leaving evaporator
5	liquid leaving evaporator

Greek Letters

η_v volumetric efficiency of compressor, %
Δ incremental change
ρ density, kg/m^3
τ time constant, min

ACKNOWLEDGMENTS

The support of the Mechanical Engineering Department and Engineering Research Institute at Iowa State University is greatly appreciated.

REFERENCES

1. J. CHI and D. DIDION: A simulation of the transient performance of a heat pump. International Journal of Refrigeration 5 (3):(1982), pp. 176-184.
2. M. DHAR and W. SOEDEL: Transient analysis of a vapor compression refrigeration system. XV International Congress of Refrigeration, Venice, Italy (1979).
3. J. W. MACARTHUR: Transient heat pump behavior: A theoretical investigation. International Journal of Refrigeration 7 (2):(1984), pp. 128-132.
4. W. E. MURPHY and V. W. GOLDSCHMIDT: Cyclic characteristics of a typical residential air conditioner--Modeling of start-up transients. ASHRAE Transactions 91 (2):(1985).
5. W. E. MURPHY and V. W. GOLDSCHMIDT: Cycling characteristics of a residential air conditioner--Modeling of shutdown transients. ASHRAE Transactions 92(1):(1986).
6. W. F. STOECKER and J. W. JONES: Refrigeration and Air Conditioning. New York: McGraw-Hill Book Co. (1982).
7. J. L. DOOLITTLE and A. H. ZERBAN: Engineering Thermodynamics Theory and Applications. Scranton: International Textbook Co. (1964).
8. R. C. DOWNING: Refrigerant equations. ASHRAE Transactions 88(2):(1974) pp. 291-306.
9. G. W. GATECLIFF and E. R. LADY: Mathematical representation of the thermodynamic properties of Refrigerants 12 and 22 in the superheat region. XIII International Congress of Refrigeration, Washington, D.C. (1971).
10. D. D. WILE: The measurement of expansion valve capacity. Refrigeration Engineering 30 (2):(1935), pp. 79-83.
11. F. J. HALE: Introduction to Control System Analysis and Design. Englewood Cliffs: Prentice-Hall Inc. (1970).
12. W. M. KAYS and A. L. LONDON: Compact Heat Exchangers. New York: McGraw-Hill Book Co. (1984).
13. W. W. AKERS and H. F. ROSSON: Condensation inside a horizontal tube. Chemical Engineering Progress Symposium Series 55 (29):(1959), pp. 145-149.
14. S. S. KANDLIKAR: An improved correlation for predicting two-phase flow boiling heat transfer coefficient in horizontal and vertical tubes. 21st National Heat Transfer Conference, Seattle, WA, July (1983); in Heat Exchangers for Two-Phase Flow Applications, ASME, New York (1983).
15. N. RAJENDRAN: A computer model of the start-up transients in a vapor compression refrigeration system. M.S. Thesis, Iowa State University (1985).
16. W. J. MULROY and D. A. DIDION: Refrigerant migration in a split-unit air conditioner. ASHRAE Transactions 91(1A):(1985), pp. 193-206.

RESUME

Le but de cette étude a été de mettre au point une maquette et un programme informatique pour simuler l'évolution du comportement d'un système de compression de vapeur lors de sa mise en route, puis d'analyser un cas typisque en utilisant le programme informatique. Le matériel d'essai conçu pour cette étude comprend des maquettes pour représenter le condensateur, l'évaporateur, le compresseur, le système de dilatation et l'accumulateur. Le réfrigérant dans chaque composant est représentré par un système simplifié avec seulement un point de mesure dans chaque partie de l'appareil. Les équations de conservation de masse et d'énergie du réfrigérant à l'intérieur de l'accumulateur, dans la cage de compression, et dans chaque échangeur de chaleur sont exprimées sous la forme de différentielles. Les équations d'énergie ont également été notées, pour ce qui est du matériau de construction de chacun des composants cités ci-dessus. C'est par des méthodes numériques que l' on a résolu toute une série d'équations différencielles traditionnelles.

Un essai de programme informatique est présenté ici et les résultats sont conformes aux hypothèses émises en ce qui concerne le comportement du système. Celles-ci etaient fondées sur des comparaisons avec des modèles d'essai antérieurs et le peu de données expérimentales existantes. De rapides fluctuations dans les variables du système son apparues tout de suite après la mise en route. Le système atteignit son état normal de marche environ 12 minutes et demi après, et seulement après que le liquide dans l'accumulateur eut séché. Immediâtement après la mise en route, on a pu observer que le réfrigérant se déplaçait de la partie à basse pression vers celle à haute pression.